

## **Surveillance of densoviruses and mesomycetozoans inhabiting grossly normal tissues of three New Zealand asteroid species**

Ian Hewson<sup>1\*</sup> and Mary A. Sewell<sup>2</sup>

<sup>1</sup>Department of Microbiology, Cornell University

<sup>2</sup>School of Biological Sciences, University of Auckland

Original Paper for Submission to *PLoS One*

\*Corresponding Author

Department of Microbiology

Wing Hall 403

Cornell University

Ithaca NY 14853

USA

[hewson@cornell.edu](mailto:hewson@cornell.edu)

1 **ABSTRACT**

2 Asteroid wasting events and mass mortality have occurred for over a century. We currently lack  
3 a fundamental understanding of the microbial ecology of asteroid disease, with disease  
4 investigations hindered by sparse information about the microorganisms associated with grossly  
5 normal specimens. We surveilled viruses and protists associated with grossly normal specimens  
6 of three asteroid species (*Patiriella regularis*, *Stichaster australis*, *Coscinasterias muricata*) on  
7 the North Island, New Zealand, using metagenomes prepared from virus and ribosome-sized  
8 material. We discovered several densovirus-like genome fragments in our RNA and DNA  
9 metagenomic libraries. Subsequent survey of their prevalence within populations by quantitative  
10 PCR (qPCR) demonstrated their occurrence in only a few (13 %) specimens (n = 36). Survey of  
11 large and small subunit rRNAs in metagenomes revealed the presence of a mesomycete (most  
12 closely matching *Ichthyosporea* sp.). Survey of large subunit prevalence and load by qPCR  
13 revealed that it is widely detectable (80%) and present predominately in body wall tissues across  
14 all 3 species of asteroid. Our results raise interesting questions about the roles of these  
15 microbiome constituents in host ecology and pathogenesis under changing ocean conditions.

16

17 **KEYWORDS:** Densovirus, Mesomycetozoa, Asteroid, Disease, Echinoderm

## 18 INTRODUCTION

19 Recent and renewed interest in echinoderm microbiome ecology has revealed the paucity in  
20 understanding of the roles of the microbial community in host biology and ecology; particularly  
21 with respect to negative impacts such as mass mortality. Asteroid mass mortality due to a  
22 condition termed “sea star wasting disease” (also known as “asteroid idiopathic wasting  
23 syndrome”) has occurred in the northeast Pacific starting in 2013 [1], and in Port Phillip Bay,  
24 Australia and Shandong Province, China in 2014 [2]. Indeed, wasting has been observed for over  
25 a century [3]. Microbiological investigation of wasting asteroids initially indicated the presence  
26 of the Asteroid ambidensovirus 1 [4] (known at the time as Sea Star associated Densovirus or  
27 SSaDV; [1]), and wasted asteroids were inhabited by a suite of cultivable copiotrophic (i.e.  
28 bacteria that rapidly consume abundant organic matter) bacteria [5, 6]. Firm microbial  
29 associations with sea star wasting remain elusive, similar to other echinoderm diseases (reviewed  
30 in [7]). Despite the lack of conclusive disease etiology, previous work has highlighted distinct  
31 microbiome associations with echinoderms [8], building on previous microscopic and  
32 cultivation-based studies [9-11]. These surveys suggest that echinoderms may harbor an  
33 underexplored diversity of microorganisms. Environmental perturbation under future climate  
34 scenarios may shift the relationship between these microorganisms and their hosts [12]. Hence,  
35 there is value in surveying the diversity and prevalence of microorganisms associated with  
36 grossly normal specimens, which may then inform future marine disease event investigations,  
37 when and if they occur.

38 A grand challenge in surveying microbial eukaryotic microorganisms associated with metazoa  
39 using PCR-based approaches is that well-conserved marker genes (e.g. ribosomal RNAs) are  
40 shared between symbiotic partners. Hence, unbiased surveys of host-associated protists using  
41 PCR amplification-based approaches are limited. Modified primer design to exclude metazoan  
42 partners, using primers distinct to expected taxonomic groups (e.g. fungal ITS; [13]), and the use  
43 of blocking PCR primers [14, 15] may alleviate this burden, but demand *a priori* knowledge of  
44 native protistan diversity. The study of viral diversity associated with metazoan hosts has been  
45 approached by two methods. First, viral genomes have been recovered from deeply sequenced  
46 host transcriptomes [16, 17]. This approach provides key information about expressed host genes  
47 in addition to a wealth of viral diversity, including deeply-branching viral genotypes across a

48 wide range of invertebrate hosts [17]. A second approach enriches for viruses by physical size  
49 and capsid-induced protection from nucleases [18]. Here, viral metagenomes are typically  
50 prepared using a homogenization-size exclusion-nuclease approach, where tissues are normally  
51 ‘cleaned’ (washed) of putative epibionts [19]. Viral metagenomes prepared using this approach  
52 have potential to yield more information than viruses alone, since only a tiny fraction (typically <  
53 5%) of metavirome sequence space is annotated as viruses [20] and the remaining sequence  
54 space is believed to mostly reflect host RNAs. Ribosomes, which are typically 25 – 30 nm in  
55 diameter, are also liberated from cells during homogenization, pass through the filters typically  
56 used in metavirome preparation, and transcript RNAs may be protected from nucleases used to  
57 digest co-extracted nucleic acids. Thus, ribosomal RNAs are well represented in viral  
58 metagenomes and may include protistan, bacterial and archaeal components of the host-  
59 associated microbiome. Comparison of non-viral sequences in viral metagenomes against rRNA  
60 databases can be used to study microbiome constituents that are inaccessible or impractically  
61 studied by PCR-based approaches.

62 The goal of the present study was to identify viruses and protists in common New Zealand  
63 asteroids by surveying virus- and ribosome-sized RNAs, and use this information to guide survey  
64 of microbial prevalence within and between populations and between tissue types. We  
65 discovered several densovirus genome fragments in two species of asteroid, but these were only  
66 detected at low prevalence within the populations studied by quantitative PCR. We also  
67 discovered fungal, mycetozoan and mesomycetozoan constituents of the asteroid microbiome. A  
68 mesomycetozoan similar to a fish pathogen was prevalent in all asteroids tested, and bore highest  
69 loads in body wall samples, suggesting it may be a common constituent of the asteroid  
70 microbiome.

## 71 MATERIALS AND METHODS

72 *Sample collection:* Asteroid samples (n = 77 individuals across 3 species) were collected for  
73 metagenomic investigation of viral diversity and viral prevalence at several locations on the  
74 North Island, New Zealand, in January and February 2018 (Table 1). Asteroids were collected by  
75 hand, either from the intertidal or subtidal, and immediately placed into individual plastic bags,  
76 which were transported to the laboratory for dissection in a cooler (Fig. 1). The taxonomic  
77 identity and arm length of individuals was recorded for each specimen. Coelomic fluid was  
78 withdrawn from individuals using a 5 mL syringe fitted with a sterile 25G needle. Body wall  
79 tissues were removed by sterile (5 mm) biopsy punch. Gonads and pyloric caeca were dissected  
80 from coelomic cavities by first creating an incision into the coelomic cavity using clean  
81 disposable razor blades, then using sterilized forceps to remove small (~ 2 – 4 mm) sections of  
82 these tissues. All tissue and coelomic fluid samples were preserved in RNALater at a ratio of 2:1  
83 (vol:vol), refrigerated, and transported to the laboratory at Cornell University for further  
84 processing, which occurred within 4 months of collection.

85 **Figure 1:** Sampled specimens of *Stichaster australis* (A-B), *Coscinasterias muricata* (C-D) and  
86 *Patiriella regularis* (E-F). Viral metagenomes were prepared from body wall (b) samples  
87 collected by biopsy punch. Additional specimens of gonad (g) and pyloric caeca (p) were  
88 collected for quantification of viral genotypes and the mesomycetozoan.

89 **Table 1:** Sampling locations, species and morphological characteristics of asteroids collected as  
90 part of this study. Samples collected at Ti Point were collected subtidally by SCUBA Diver,  
91 while those collected elsewhere were collected intertidally. RL = Ray length, SE = Standard  
92 Error.

Location	Latitude	Longitude	Date	Species	n	RL (cm)	RL SE
Piha, Auckland	36.9597 S	174.4628 E	1/22/2018	<i>Stichaster australis</i>	19	13.58	0.56
Ti Point, Northland	36.3178 S	174.6178 E	1/27/2018	<i>Coscinasterias muricata</i>	17	7.42	1.10
Matheson's Bay, Northland	36.3011 S	171.8011 E	1/27/2018	<i>Patiriella regularis</i>	20	2.81	0.17

				<i>Coscinasterias muricata</i>	1	10.00	
Scorcher Bay, Wellington	41.3078 S	174.8325 E	2/15/2018	<i>Patiriella regularis</i>	20	1.89	0.11

93

94 *Metavirome Preparation:* Three body wall biopsy samples from each species were selected for  
95 viral metagenomics (one each from *Stichaster australis*, *Coscinasterias muricata* and *Patiriella*  
96 *regularis*; Table 2). For each sample, the biopsy punch was removed from RNALater and subject  
97 to the workflow detailed in [19] with modifications by Ng et al [21] and Hewson et al. [22].  
98 Briefly, the sample was homogenized by bead beating (Zymo Bead Beater tubes) in 1 mL of 0.02  
99  $\mu$ m-filtered PBS. The sample was filtered through a 0.2  $\mu$ m PES syringe filter. The filtrate was  
100 treated with DNase I (5 U; Thermo Fisher Scientific), RNase One (50 U; Promega) and  
101 Benzonase (250 U; Sigma-Aldrich) for 3 h at 37°C in an attempt to remove co-extracted host  
102 nucleic acids. Enzyme activity was halted by treatment with 50  $\mu$ M EDTA. RNA was extracted  
103 from the resulting purified viral fraction using the Zymo Mini RNA isolation kit, and  
104 subsequently amplified using the TransPlex WTA2 (Sigma Aldrich) kit. We did not standardize  
105 template quantity of extracted RNA (2  $\mu$ l) prior to amplification. Amplicons were quantified  
106 using PicoGreen and submitted for sequencing on a Illumina MiSeq (2 x 250 bp paired-end)  
107 platform after TruSeq PCR-free library preparation at the Cornell Biotechnology Resource  
108 Center. Sequences have been deposited in the NCBI under BioProject PRJNA636826.

109

110 **Table 2:** Library characteristics prepared from asteroids in Northland and Auckland region,  
111 January 2018.

Species	Date	Total Reads	Assembled Reads	Total Contigs	Viral Contigs
<i>Coscinasterias muricata</i>	1/27/2018	3,867,602	981,140	27,032	2
<i>Stichaster australis</i>	1/22/2018	1,673,102	681,086	2,170	0
<i>Patiriella regularis</i>	1/27/2018	1,635,372	301,574	6,332	2

115

116 *Bioinformatic processing:* Sequence libraries were initially trimmed for adapters and quality  
117 (ambiguous bases <2) using the CLC Genomics Workbench 4.0. Each of the 3 metaviromes were

118 assembled separately using the CLC Genomic Workbench 4.0 native algorithm using a minimum  
119 overlap of 0.5 and similarity of 0.8. The resulting contig spectra was aligned against several  
120 boutique databases of RNA viruses as described elsewhere [22]. Because RNA viral  
121 metagenomes also capture ssDNA viruses [23], we also searched contig spectra by tBLASTx  
122 against a boutique database of densoviral genomes (complete genomes from NCBI using  
123 keyword “densovirus”). Sequence matches against any of these databases at an E-value  $<10^{-20}$   
124 were further aligned against the non-redundant (nr) library at NCBI by BLASTx, and contigs  
125 discarded if they matched known bacterial or eukaryl proteins at a higher percentage and E-value  
126 than viruses. Uncertain amplification biases and variation in template RNA quantity preclude  
127 quantitative interpretation of metagenome constituents. Hence, analyses of metagenomes focused  
128 on detection of constituents and subsequent quantitative PCR of selected contigs.

129 *Quantitative PCR (qPCR) of densovirus genome fragments:* TaqMan Primer/Probe sets were  
130 designed around two contiguous sequences matching the nonstructural proteins of densoviruses  
131 (*Coscinasterias muricata* contig 17 and *Patiriella regularis* contig 15838) and validated against  
132 an oligonucleotide standard (Table 2). DNA was extracted from 36 biopsy punch body wall  
133 samples (10 *Stichaster australis*, 3 *Coscinasterias muricata*, 13 *Patiriella regularis* from near  
134 Auckland and 10 *Patiriella regularis* from Scorch Bay, Wellington) using the Zymo Tissue &  
135 Insect Kit. DNA was then subject to quantitative PCR (qPCR) in an Applied Biosystems  
136 StepOne Real-Time PCR machine. Each qPCR reaction comprised 1 X SSO Probes SuperMix  
137 (BioRad), and 200 pmol of each primer and probe (Table 2). Reactions were subject to a 10  
138 minute incubation step at 50°C, followed by a 3 minute denaturation step at 94°C. Following hot  
139 start activation, reactions were subject to 50 cycles of heating to 94°C and annealing at 58°C,  
140 where fluorescence was measured at the conclusion of each thermal cycle. Reactions were run in  
141 duplicate against an 8-fold dilution (covering 10 to  $10^8$  copies reaction<sup>-1</sup>). A positive detection of  
142 the virus was considered when both duplicates were within 1 Ct, and were considered “detected  
143 but not quantifiable” (DNQ) when one replicate generated a positive Ct but the other replicate  
144 failed to yield an amplicon.

145

146

147 **Table 3:** Primers and probes used in this study to examine the prevalence and load of densovirus  
148 and mesomycetozoan-like contiguous sequences.

Target	Primer Name	Sequence (5' - 3')
<i>Patiriella regularis</i> contig 15838	NZ1DV_F	AGTTGTTACTTGGGGCTTGT
	NZ1DV_R	CCGTGCTCAGTACTTGTCTG
	NZ1DV_Pr	[FAM]CAGCACCAAGATGTTGCAGCTGTTGA[TAM]
	NZ1DV_Std	AGTTGTTACTTGGGGCTTGTATAATAACTGCTACAGCACCAAGATGTTGCAGCTGTTGATCAAGTTAATGCACGACAAAGTACTGAGCACGG
<i>Coscinasterias muricata</i> contig 17	NZ3DV_F	ATCTTCAATGCACTCGGAGC
	NZ3DV_R	AGTAACGCCATGGATCTCGA
	NZ3DV_Pr	[FAM]AGTGTACAGAACGCGCTTGTGGA[TAM]
	NZ3DV_Std	ATCTTCAATGCACTCGGAGCCAGTGTACAGAACGCGCTTGTGGAAC TACAAGCACAAATCAGAATTGAGATCCATGGCGTTACT
<i>Stichaster australis</i> contig 929	NZ2Iso_F	GCTAGGGTTCTATGGCTGGT
	NZ2Iso_R	GCTCCCCAGGATTTCAAGG
	NZ2Iso_Pr	[FAM]CGAGTCCGGTGCCTCGA[TAM]
	NZ2Iso_Std	GCTAGGGTTCTATGGCTGGTAGAGCTGGCACTTCTGCCGAGTCCGG TGCGTCCTCGACGGCCCTGAAAATCCTGGGGAGC

149

150 *Investigation of eukaryote 18S and 28S rRNAs in metaviromes:* Contiguous sequences generated  
151 from viral metagenomes (described above) were queried against the Silva database (version  
152 r132) of 16S/18S and 23S/28S rRNAs [24] by BLASTn and contigs matching at E<10<sup>-10</sup> to 18S  
153 or 28S rRNAs were considered for further analysis. Matches meeting this criterion were then  
154 queried against the non-redundant database at NCBI. Matches to asteroid 18S and 28S rRNAs  
155 were removed from further consideration, as were matches to other metazoan rRNAs. The  
156 resulting contig spectra were aligned against close matches from NCBI using the CLC Sequence  
157 Viewer 8.0 (Qiagen).

158 *Investigation of mesomycetozoan tissue and species specificity:* Quantitative PCR (qPCR)  
159 primers were designed around the 28S rRNA sequence matching *Ichthyosporea* sp. (*Stichaster*  
160 contig 929) and used to amplify body wall DNA extracts from 20 *Stichaster australis*, 6  
161 *Coscinasterias muricata*, and 10 *Patiriella regularis*. Additionally, for each of the 20 *Stichaster*

162 *australis*, samples of pyloric caeca and gonad were also examined for the presence and  
163 abundance of this sequence.

164

## 165 RESULTS AND DISCUSSION

166 *Viruses associated with Asteroid Tissues*: Metaviromes prepared from asteroid body wall  
167 samples contained between 1.6 – 3.9 million paired-end reads (Table 2). Assembly of these  
168 resulted in 2,170 to 27,032 contigs, where contigs recruited 18 – 41% of total reads. No RNA  
169 viruses were detected by alignment. However, alignment against densoviral genomes resulted in  
170 2 contigs matching to the nonstructural gene 1 (NS1) and 2 contigs matching structural (VP)  
171 genes at  $E < 10^{-15}$  (Fig. 2). Three of these contigs – two from *Coscinasterias muricata* and one  
172 from *Patiriella regularis*- overlapped with ambidensovirus peptide sequences recovered from  
173 species of starfish collected worldwide. A further contig from *Patiriella regularis* matched a  
174 decapod penstyldensoviruses. Phylogenetic analyses based on NS1 revealed that *Coscinasterias*  
175 *muricata* contig 16413 was most similar to densovirus recovered from *Asterias rubens* in  
176 Scotland [25] (Fig. 3). Phylogenetic analyses based on structural genes of the remaining viral  
177 contigs (*Coscinasterias muricata* contig 15838 and *Patiriella regularis* contig 3718) suggested  
178 that these were most similar to ambidensovirus from molluscs [26, 27], insects [28], a  
179 crustacean [29], and human spinal fluid [30]. Quantitative PCR (qPCR) of the densovirus-like  
180 *Coscinasterias muricata* contig 15838 yielded only 3 DNQ results; two in *Coscinasterias*  
181 *muricata* (of 3 total surveyed) from Ti Point; and one *Stichaster australis* from Piha. qRT-PCR  
182 of *Patiriella* contig 17 yielded two DNQ results, both from *Patiriella regularis* collected at  
183 Matheson's Bay. In no sample did we consistently detect the presence of either contig between  
184 replicate amplifications. This may be interpreted as indicating their very low copy number (<10)  
185 in DNA extracts.

186 **Figure 2:** Contig map of densovirus-like genome fragments recovered from *Coscinasterias*  
187 *muricata* and *Patiriella regularis* viral metagenomes. The colors of arrows indicate densoviral  
188 gene, and the best match (by BLASTx against the non-redundant database at NCBI) along with  
189 e-value is indicated adjacent to each ORF. The black lines running through ORFs indicate total  
190 contig length. The numbers in brackets below each contig are the number of reads recruiting to  
191 the contig from the origin library.

192 **Figure 3:** Phylogenetic representation of *Patiriella regularis* and *Coscinasterias muricata*-  
193 associated densoviral genome fragments. The trees are based upon 170 amino acid (Non-  
194 Structural), 211 amino acid (Structural; middle), and 104 amino acid (Structural; bottom)  
195 alignments performed using the CLC Sequence Viewer version 8.0. The trees were constructed  
196 with neighbor joining and Jukes-Cantor distance, where bootstrap values (1000 reps) are  
197 indicated above nodes. Red labels indicate sequences obtained in this study, while green labels  
198 indicate sequences obtained from asteroids in other studies.

199

200 The observation of densovirus in these species was not surprising, since their recovery in other  
201 asteroids [1, 5, 23, 31] and urchins [32] suggests they may be a common constituent of  
202 echinoderm microbiomes. Parvoviruses form persistent infections in hosts [33, 34], and are  
203 highly prevalent and persistent in asteroid populations [31]. They are also widely endogenized in  
204 host genomes [35]. None of the densovirus-like contigs discovered in this survey represented  
205 complete genomes, so it is possible that these also represent endogenized densoviruses.  
206 However, flanking regions to their open reading frames did not match asteroid genomes,  
207 suggesting they were unlikely to be endogenized genome elements.

208 The pathology of densovirus and significance in wasting diseases or other conditions is  
209 unclear. The copy number of Asteroid ambidensovirus-1 (SSaDV) and related densoviruses is  
210 elevated in wasting-affected *Pycnopodia helianthoides* [5]. However, histopathology [36] and  
211 other investigations [6, 23, 31] have failed to clinically connect densovirus (or viruses in  
212 general) to sea star wasting disease. Densovirus, like all parvoviruses, replicate in somatic  
213 cells. Infection in arthropods leads to respiratory impairment [37] and triggering of apoptosis  
214 [38], and has been linked to elevated mortality in crustacea [29, 39]. The discovery of a  
215 penstyldensovirus genome fragment in *Patiriella regularis* raises interesting questions about its  
216 role in host ecology. In penaeid shrimp, persistent infection by penstyldensovirus delays  
217 mortality from white spot syndrome virus [40], suggesting densovirus in general may play both  
218 detrimental and beneficial roles in host ecology. None of the asteroids sampled in this survey  
219 were grossly abnormal, and the low prevalence of the *Patiriella regularis* penstyldensovirus  
220 genome fragment in asteroid populations at our collection sites may indicate that these infections

221 represent sub-clinical, or perhaps persistent infections which are unrelated to wasting or mass  
222 mortality.

223 *Protists associated with asteroids:* A total of 15 contigs matched 18S and 28S rRNAs based on  
224 alignment. Of these, nine were fungal (five were Ascomycetes, four were Basidiomycetes), two  
225 were mycetozoan and one was mesomycetozoan (Fig. 4; Figs. S1-S4). The mesomycetozoan  
226 contiguous sequence (*Stichaster* contig 929) was most similar to a fish pathogen *Ichthyosporea*  
227 sp. ex *Tenebrio molitor* (Fig. 4). The abundance of this contiguous sequence was significantly  
228 higher in the body wall of *Stichaster australis* than in either *Coscinasterias muricata* ( $p = 0.019$ ,  
229 Student's t-test,  $df=4$ ) or *Patiriella regularis* ( $p = 0.018$ , Student's t-test,  $df=4$ ) (Fig. 5). The  
230 abundance in epidermal tissues was also significantly higher in *Stichaster australis* than in either  
231 gonads or pyloric caeca ( $p = 0.013$  and  $p=0.006$ , respectively, Student's t-test,  $df=8$ ). The  
232 contiguous sequence was detected in any quantity in 80 – 85% of all samples tested with no  
233 pattern with tissue specificity or species.

234

235 **Fig. 4:** Phylogenetic representation of asteroid-associated 28S rRNA sequences in purified virus  
236 metagenomes. The tree was constructed by neighbor joining and based on an 849 nucleotide  
237 alignment of eukaryotic 28S rRNA. Shown are close matches by BLAST against the non-  
238 redundant database.

239

240 **Fig. 5:** Mesomycetozoan 28S rRNA copies as determined by qPCR in asteroid tissues. a,b  
241 denotes significant difference ( $p < 0.025$ , Student's t-test with Bonferroni correction for 2  
242 comparisons).

243

244 The association of microbial eukaryotes, especially fungi and fungi-like protists, with  
245 echinoderms is not extensively documented in previous surveys. Hewson et al [22] reported the  
246 detection of totiviruses, which are fungal viruses, in several Holothuroidea. Similarly, Nerva et al  
247 [41] reported the mycovirome of fungi isolated from *Holothuria polii*. These reports suggest that  
248 fungi may be common constituents of the sea cucumber microbiome. Wei et al [42] reported the  
249 cultivation of a symbiotic fungi most similar to *Penicillium* from an asteroid in China.  
250 Labyrinthulids have also been cultivated from the surface of wasting asteroids in the northeast

251 Pacific [43]. However, their role in wasting pathology is unknown. There has been a body of  
252 work examining anti-fungal properties of asteroid extracts [44-47], suggesting that fungi  
253 discovered in this survey are unlikely to represent pathogens, but rather may be adapted to the  
254 chemical environment of their host. Further investigation of their roles in host chemical defense  
255 and dysbiosis is therefore warranted.

256 Mesomycetozoa are of interest since they represent the closest unicellular ancestor to  
257 multicellular animals [48]. They represent parasites of vertebrates [49-51] of which several,  
258 including *Ichthyosporea* spp. are aquatic. Aquatic mesomycetozoans infect fish and amphibians  
259 [50-53] and cause dermal disease. Mesomycetozoa may also form symbioses with their hosts  
260 (e.g. the mealworm *Tenebrio molitor*; [54] and other taxa [55, 56] (reviewed in [57]). Our  
261 observation of an *Ichthyosporea*-like rRNA in *Stichaster* is the first report of this group in  
262 Asteroidea. The observations of greater load in epidermal tissues than internal organs suggests  
263 they may also form dermal infections, and their widespread occurrence in asteroid populations  
264 from the North Island of New Zealand suggests that mesomycetozoans are non-specific and  
265 broadly prevalent. Because we did not observe gross disease signs in any specimen, it is unlikely  
266 that this microorganism is a pathogen, but rather, they may represent a normal constituent of the  
267 host microbiome.

268

## 269 CONCLUSIONS

270 To the best of our knowledge, this is the first investigation of viruses and mesomycetozoa  
271 associated with asteroids in New Zealand. Discovery of these taxa suggests an undiscovered  
272 bank of potential parasites or symbionts inhabiting echinoderms, and demands further  
273 investigation into their ecological roles. While we did not observe gross signs of disease in any  
274 specimen, we speculate that they may cause sub-clinical disease, or may interact with changing  
275 ocean conditions and give rise to more extensive disease events in the future. Our work  
276 demonstrates the value in unbiased surveys of microbiome constituents (i.e. microbial  
277 surveillance) which may inform future disease investigations by providing a picture of grossly  
278 normal microbiome constituents.

279

280 **ACKNOWLEDGEMENTS**

281 The authors thank Richard Taylor for sample collection at Ti Point, and Christopher DeRito,  
282 Elliot Jackson and Kalia Bistolas for assistance with laboratory analyses. This work was  
283 supported by the United States National Science Foundation grants OCE- 1737127 and OCE-  
284 1537111 to IH. The datasets generated during the current study are available in the NCBI  
285 repository under BioProject PRJNA636826.

286

287 **REFERENCES**

- 288 1. Hewson I, Button JB, Gudenkauf BM, Miner B, Newton AL, Gaydos JK, et al.  
289 Densovirus associated with sea-star wasting disease and mass mortality. *Proc Nat Acad Sci*  
290 USA. 2014;111:17276-83.
- 291 2. Hewson I, Sullivan B, Jackson EW, Xu Q, Long H, Lin C, et al. Perspective: Something  
292 old, something new? Review of wasting and other mortality in Asteroidea (Echinodermata).  
293 *Front Mar Sci.* 2019;6(406). doi: 10.3389/fmars.2019.00406.
- 294 3. Mead AD. Twenty-eighth annual report of the commissioners of inland fisheries, made to  
295 the General Assembly at its January session, 1898. Providence: 1898.
- 296 4. Walker PJ, Siddell SG, Lefkowitz EJ, Mushegian AR, Dempsey DM, Dutilh BE, et al.  
297 Changes to virus taxonomy and the International Code of Virus Classification and Nomenclature  
298 ratified by the International Committee on Taxonomy of Viruses (2019). *Archiv Virol.*  
299 2019;164(9):2417-29. doi: 10.1007/s00705-019-04306-w.
- 300 5. Hewson I, Bistolas KSI, Quijano Carde EM, Button JB, Foster PJ, Flanzenbaum JM, et  
301 al. Investigating the complex association between viral ecology, environment and Northeast  
302 Pacific Sea Star Wasting. *Front Mar Sci.* 2018;<https://doi.org/10.3389/fmars.2018.00077>.
- 303 6. Aquino CA, Besemer RM, DeRito CM, Kocian J, Porter IR, Raimondi PT, et al.  
304 Evidence that non-pathogenic microorganisms drive sea star wasting disease through boundary  
305 layer oxygen diffusion limitation. *bioRxiv.* 2020:doi: <https://doi.org/10.1101/2020.07.31.231365>
- 306 7. Hewson I. Technical pitfalls that bias comparative microbial community analyses of  
307 aquatic disease. *Dis Aquat Organ.* 2019;137(2):109-24. doi: 10.3354/dao03432.

308 8. Jackson EW, Pepe-Ranney C, Debenport SJ, Buckley DH, Hewson I. The microbial  
309 landscape of sea stars and the anatomical and interspecies variability of their microbiome. *Front*  
310 *Microbiol.* 2018;9:12. doi: 10.3389/fmicb.2018.01829.

311 9. Kelly MS, Barker MF, McKenzie JD, Powell J. The incidence and morphology of  
312 subcuticular bacteria in the echinoderm fauna of New Zealand. *Biol Bull.* 1995;189(2):91-105.  
313 doi: 10.2307/1542459.

314 10. Kelly MS, McKenzie JD. Survey of the occurrence and morphology of sub-cuticular  
315 bacteria in shelf echinoderms from the northeast Atlantic Ocean. *Mar Biol.* 1995;123(4):741-56.  
316 doi: 10.1007/bf00349117.

317 11. Holland ND, Nealson KH. Fine structure of the echinoderm cuticle and the sub-cuticular  
318 bacteria of echinoderms. *Acta Zool.* 1978;59(3-4):169-85. doi: 10.1111/j.1463-  
319 6395.1978.tb01032.x.

320 12. Egan S, Gardiner M. Microbial dysbiosis: Rethinking disease in marine ecosystems.  
321 *Front Microbiol.* 2016;7. doi: 10.3389/fmicb.2016.00997.

322 13. Nuñez-Pons L, Work TM, Angulo-Preckler C, Moles J, Avila C. Exploring the pathology  
323 of an epidermal disease affecting a circum-Antarctic sea star. *Sci Rep.* 2018;8:12. doi:  
324 10.1038/s41598-018-29684-0.

325 14. Leray M, Agudelo N, Mills SC, Meyer CP. Effectiveness of annealing blocking primers  
326 versus restriction enzymes for characterization of generalist diets: unexpected prey revealed in  
327 the gut contents of two coral reef fish species. *PLoS One.* 2013;8(4):e58076-e. doi:  
328 10.1371/journal.pone.0058076.

329 15. Vestheim H, Jarman SN. Blocking primers to enhance PCR amplification of rare  
330 sequences in mixed samples - a case study on prey DNA in Antarctic krill stomachs. *Front Zool.*  
331 2008;5:12-. doi: 10.1186/1742-9994-5-12.

332 16. Holmes EC. The expanding virosphere. *Cell Host Microbe.* 2016;20(3):279-80.

333 17. Shi M, Lin X-D, Tian J-H, Chen L-J, Chen X, Li C-X, et al. Redefining the invertebrate  
334 RNA virosphere. *Nature.* 2016;540:539-43.

335 18. Ng TFF, Manire C, Borrowman K, Langer T, Ehrhart L, Breitbart M. Discovery of a  
336 novel single-stranded DNA virus from a sea turtle fibropapilloma by using viral metagenomics. *J*  
337 *Virol.* 2009;83(6):2500-9. doi: Doi 10.1128/Jvi.01946-08.

338 19. Thurber RV, Haynes M, Breitbart M, Wegley L, Rohwer F. Laboratory procedures to  
339 generate viral metagenomes. *Nat Protocol*. 2009;4(4):470-83. doi: DOI 10.1038/nprot.2009.10.

340 20. Correa AMS, Welsh RM, Thurber RLV. Unique nucleocytoplasmic dsDNA and +ssRNA  
341 viruses are associated with the dinoflagellate endosymbionts of corals. *ISME J*. 2013;7(1):13-27.

342 21. Ng FFT, Wheeler E, Greig D, Waltzek TB, Gulland F, Breitbart M. Metagenomic  
343 identification of a novel anellovirus in Pacific harbor seal (*Phoca vitulina richardsii*) lung  
344 samples and its detection in samples from multiple years. *J Gen Virol*. 2011;92(6):1318-23. doi:  
345 10.1099/vir.0.029678-0.

346 22. Hewson I, Johnson MR, Tibbetts IR. An unconventional flavivirus and other RNA  
347 viruses in the sea cucumber (Holothuroidea; Echinodermata) virome. *Viruses*. 2020;12:1057.

348 23. Jackson EW, Wilhelm RC, Johnson MR, Lutz HL, Danforth I, Gaydos JK, et al.  
349 Diversity of sea star-associated densoviruses and transcribed endogenized viral elements of  
350 densovirus origin. *J Virol*. 2020;DOI: 10.1128/JVI.01594-20. doi: 10.1101/2020.08.05.239004.

351 24. Quast C, Pruesse E, Yilmaz P, Gerken J, Schweer T, Yarza P, et al. The SILVA  
352 ribosomal RNA gene database project: improved data processing and web-based tools. *Nucleic  
353 Acids Res*. 2012;41(D1):D590-D6. doi: 10.1093/nar/gks1219.

354 25. Waldron FM, Stone GN, Obbard DJ. Metagenomic sequencing suggests a diversity of  
355 RNA interference-like responses to viruses across multicellular eukaryotes. *PLOS Genetics*.  
356 2018;14(7):e1007533. doi: 10.1371/journal.pgen.1007533.

357 26. Kang YJ, Huang W, Zhao AL, Lai DD, Shao L, Shen YQ, et al. Densoviruses in oyster  
358 *Crassostrea ariakensis*. *Arch Virol*. 2017;162(7):2153-7. Epub 2017/03/28. doi:  
359 10.1007/s00705-017-3343-z. PubMed PMID: 28342032.

360 27. Richard JC, Leis E, Dunn CD, Agbalog R, Waller D, Knowles S, et al. Mass mortality in  
361 freshwater mussels (*Actinonaia pectorosa*) in the Clinch River, USA, linked to a novel  
362 densovirus. *Sci Rep*. 2020;10(1):14498. doi: 10.1038/s41598-020-71459-z.

363 28. Guo H, Zhang J, Hu Y. Complete sequence and organization of *Periplaneta fuliginosa*  
364 densovirus genome. *Acta Virol*. 2000;44(6):315-22.

365 29. Bochow S, Condon K, Elliman J, Owens L. First complete genome of an  
366 Ambidensovirus; *Cherax quadricarinatus* densovirus, from freshwater crayfish *Cherax*  
367 *quadricarinatus*. *Mar Genomics*. 2015;24 Pt 3:305-12. Epub 2015/08/14. doi:  
368 10.1016/j.margen.2015.07.009.

369 30. Phan TG, Messacar K, Dominguez SR, da Costa AC, Deng X, Delwart E. A new  
370 densovirus in cerebrospinal fluid from a case of anti-NMDA-receptor encephalitis. *Arch Virol*.  
371 2016;161(11):3231-5. Epub 2016/08/16. doi: 10.1007/s00705-016-3002-9.

372 31. Jackson EW, Pepe-Ranney C, Johnson MR, Distel DL, Hewson I. A highly prevalent and  
373 pervasive densovirus discovered among sea stars from the north american Atlantic coast. *Appl*  
374 *Environ Microbiol*. 2020;86(6). doi: 10.1128/AEM.02723-19.

375 32. Gudenkauf BM, Eaglesham JB, Aragundi WM, Hewson I. Discovery of urchin-  
376 associated densoviruses (Parvoviridae) in coastal waters of the Big Island, Hawaii. *J Gen Virol*.  
377 2014;95:652-8.

378 33. Frickhofen N, Young NS. Persistent parvovirus B19 infections in humans. *Microb*  
379 *Pathogen*. 1989;7(5):319-27. doi: [https://doi.org/10.1016/0882-4010\(89\)90035-1](https://doi.org/10.1016/0882-4010(89)90035-1).

380 34. Molthathong S, Jitrakorn S, Joyjinda Y, Boonchird C, Witchayachamnarkul B,  
381 Pongtippatee P, et al. Persistence of *Penaeus stylirostris* densovirus delays mortality caused by  
382 white spot syndrome virus infection in black tiger shrimp (*Penaeus monodon*). *BMC Vet Res*.  
383 2013;9(1):33. doi: 10.1186/1746-6148-9-33.

384 35. Liu H, Fu Y, Xie J, Cheng J, Ghabrial SA, Li G, et al. Widespread endogenization of  
385 densoviruses and parvoviruses in animal and human genomes. *J Virol*. 2011;85(19):9863-76.  
386 doi: 10.1128/jvi.00828-11.

387 36. Newton AL, Smolowitz R. Chapter 41 - Invertebrates. In: Terio KA, McAloose D, Leger  
388 JS, editors. *Pathology of Wildlife and Zoo Animals*: Academic Press; 2018. p. 1019-52.

389 37. Mutuel D, Rayallec M, Chabi B, Multeau C, Salmon JM, Fournier P, et al. Pathogenesis  
390 of *Junonia coenia* densovirus in *Spodoptera frugiperda*: A route of infection that leads to  
391 hypoxia. *Virology*. 2010;403(2):137-44. doi: DOI 10.1016/j.virol.2010.04.003.

392 38. Roekring S, Smith DR. Induction of apoptosis in densovirus infected *Aedes aegypti*  
393 mosquitoes. *J Invert Pathol*. 2010;104(3):239-41. doi: DOI 10.1016/j.jip.2010.04.002.

394 39. Owens L, La Fauce K, Claydon K. The effect of *Penaeus merguiensis* densovirus on  
395 *Penaeus merguiensis* production in Queensland, Australia. *J Fish Dis*. 2011;34(7):509-15. doi:  
396 DOI 10.1111/j.1365-2761.2011.01263.x.

397 40. Molthathong S, Jitrakorn S, Joyjinda Y, Boonchird C, Witchayachamnarkul B,  
398 Pongtippatee P, et al. Persistence of *Penaeus stylirostris* densovirus delays mortality caused by

399 white spot syndrome virus infection in black tiger shrimp (*Penaeus monodon*). BMC Vet Res.  
400 2013;9. doi: Artn 33 Doi 10.1186/1746-6148-9-33.

401 41. Nerva L, Forgia M, Ciuffo M, Chitarra W, Chiapello M, Vallino M, et al. The  
402 mycovirome of a fungal collection from the sea cucumber *Holothuria polii*. Virus Res.  
403 2019;273:197737. doi: <https://doi.org/10.1016/j.virusres.2019.197737>.

404 42. Wei X, Feng C, Li XH, Mao XX, Luo HB, Zhang DM, et al. Enantiomeric polyketides  
405 from the starfish-derived symbiotic fungus *Penicillium* sp. GGF16-1-2. Chem Biodiv.  
406 2019;16(6). doi: 10.1002/cbdv.201900052.

407 43. FioRito R, Leander C, Leander B. Characterization of three novel species of  
408 Labyrinthulomycota isolated from ochre sea stars (*Pisaster ochraceus*). Mar Biol.  
409 2016;163(8):10. doi: 10.1007/s00227-016-2944-5.

410 44. Franco OP, Patino GS, Ortiz AA. Antibacterial and antifungal activity of the starfish  
411 *Oreaster reticulatus* (Valvatida: Oreasteridae) and the sea urchins *Mellita quinquesperforata*  
412 (Clypeasteroida: Mellitidae) and *Diadema antillarum* (Diadematoida: Diadematidae) from the  
413 Colombian Caribbean. Revista Biol Trop. 2015;63:329-37.

414 45. Palagiano E, Zollo F, Minale L, Iorizzi M, Bryan P, McClintock J, et al. Isolation of 20  
415 glycosides from the starfish *Henricia downeyae*, collected in the Gulf of Mexico. J Nat Prod.  
416 1996;59(4):348-54. doi: 10.1021/np9601014.

417 46. Choi DH, Shin S, Park IK. Characterization of antimicrobial agents extracted from  
418 *Asterina pectinifera*. Int J Antimicrob Agent. 1999;11(1):65-8. doi: 10.1016/s0924-  
419 8579(98)00079-x.

420 47. Chludil HD, Seldes AM, Maier MS. Antifungal steroidal glycosides from the Patagonian  
421 starfish *Anasterias minuta*: Structure-activity correlations. J Nat Prod. 2002;65(2):153-7. doi:  
422 10.1021/np010332x.

423 48. Mendoza L, Taylor JW, Ajello L. The class Mesomycetozoea: A group of  
424 microorganisms at the animal-fungal boundary. Ann Rev Microbiol. 2002;56:315-44. doi:  
425 10.1146/annurev.micro.56.012302.160950.

426 49. Baker GC, Beebee TJC, Ragan MA. *Prototheca richardsi*, a pathogen of anuran larvae, is  
427 related to a clade of protistan parasites near the animal-fungal divergence. Microbiol.  
428 1999;145:1777-84. doi: 10.1099/13500872-145-7-1777.

429 50. Fredricks DN, Jolley JA, Lepp PW, Kosek JC, Relman DA. *Rhinosporidium seeberi*: A  
430 human pathogen from a novel group of aquatic protistan parasites. *Emerg Infect Dis*.  
431 2000;6(3):273-82. doi: 10.3201/eid0603.000307.

432 51. Arkush KD, Mendoza L, Adkison MA, Hedrick RP. Observations on the life stages of  
433 *Sphaerothecum destruens* n. g., n. sp., a mesomycetozoan fish pathogen formally referred to as  
434 the rosette agent. *J Euk Microbiol*. 2003;50(6):430-8. doi: 10.1111/j.1550-7408.2003.tb00269.x.

435 52. Blazer VS, Hitt NP, Snyder CD, Snook EL, Adams CR. *Dermocystidium* sp infection in  
436 blue ridge sculpin captured in Maryland. *J Aquat Ani Health*. 2016;28(3):143-9. doi:  
437 10.1080/08997659.2016.1159622.

438 53. Arnott SA, Dykova I, Roumillat WA, de Buron I. Pathogenic endoparasites of the spotted  
439 seatrout, *Cynoscion nebulosus*: Patterns of infection in estuaries of South Carolina, USA.  
440 *Parasitol Res*. 2017;116(6):1729-43. doi: 10.1007/s00436-017-5449-3.

441 54. Lord JC, Hartzler KL, Kambhampati S. A nuptially transmitted ichthyosporean symbiont  
442 of *Tenebrio molitor* (Coleoptera: Tenebrionidae). *J Euk Microbiol*. 2012;59(3):246-50. doi:  
443 10.1111/j.1550-7408.2012.00617.x.

444 55. Marshall WL, Celio G, McLaughlin DJ, Berbee ML. Multiple isolations of a culturable,  
445 motile ichthyosporean (Mesomycetozoa, Opisthokonta), *Creolimax fragrantissima* n. gen., n. sp.,  
446 from marine invertebrate digestive tracts. *Protist*. 2008;159(3):415-33. doi:  
447 <https://doi.org/10.1016/j.protis.2008.03.003>.

448 56. Marshall WL, Berbee ML. Facing unknowns: Living cultures (*Pirum gemmata* gen. nov.,  
449 sp. nov., and *Abeloforma whisleri*, gen. nov., sp. nov.) from invertebrate digestive tracts represent  
450 an undescribed clade within the unicellular opisthokont lineage *Ichthyosporea*  
451 (Mesomycetozoa). *Protist*. 2011;162(1):33-57. doi: <https://doi.org/10.1016/j.protis.2010.06.002>.

452 57. Glockling SL, Marshall WL, Gleason FH. Phylogenetic interpretations and ecological  
453 potentials of the Mesomycetozoa (*Ichthyosporea*). *Fungal Ecol*. 2013;6(4):237-47. doi:  
454 <https://doi.org/10.1016/j.funeco.2013.03.005>.

455

## 456 SUPPORTING INFORMATION CAPTIONS

457 58. **Fig. S1:** Phylogenetic representation of asteroid-associated 18S rRNA sequences in purified  
458 virus metagenomes. The tree was constructed by neighbor joining and based on an 689

459 nucleotide alignment of eukaryotic 18S rRNAs. Shown are close matches by BLAST against the  
460 non-redundant database.

461

462 **Fig. S2:** Phylogenetic representation of asteroid-associated ascomycete 28S rRNA sequences in  
463 purified virus metagenomes. The tree was constructed by neighbor joining and based on an 368  
464 nucleotide alignment of eukaryotic 28S rRNAs. Shown are close matches by BLAST against the  
465 non-redundant database.

466

467 **Fig. S3:** Phylogenetic representation of asteroid-associated 28S rRNA sequences in purified  
468 virus metagenomes. The tree was constructed by neighbor joining and based on a 481 nucleotide  
469 alignment of eukaryotic 28S rRNAs. Shown are close matches by BLAST against the non-  
470 redundant database.

471

472 **Fig. S4:** Phylogenetic representation of asteroid-associated ascomycete 28S rRNA sequences in  
473 purified virus metagenomes. The tree was constructed by neighbor joining and based on a 506  
474 nucleotide alignment of eukaryotic 28S rRNAs. Shown are close matches by BLAST against the  
475 non-redundant database.

476

477

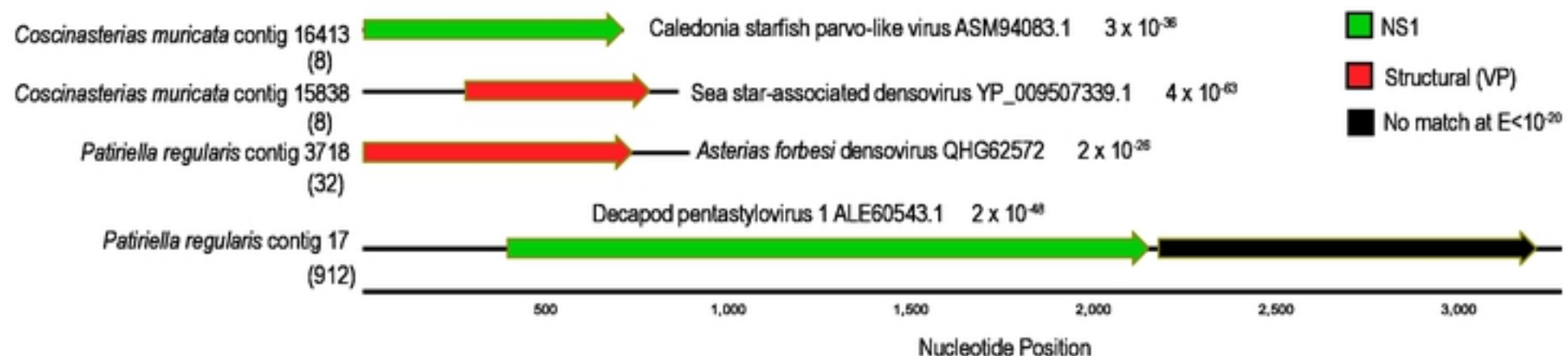


Figure 2



Figure 1

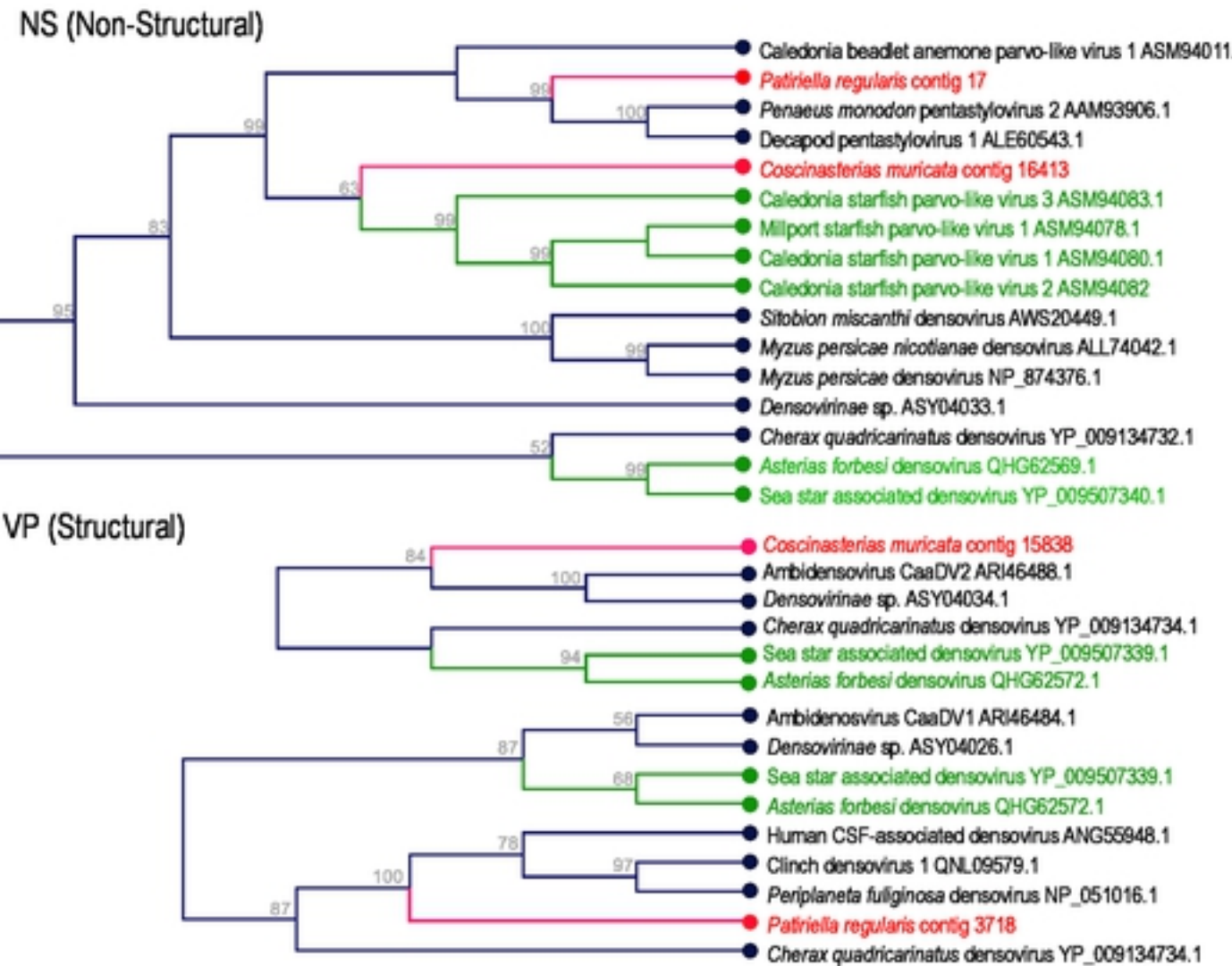


Figure 3

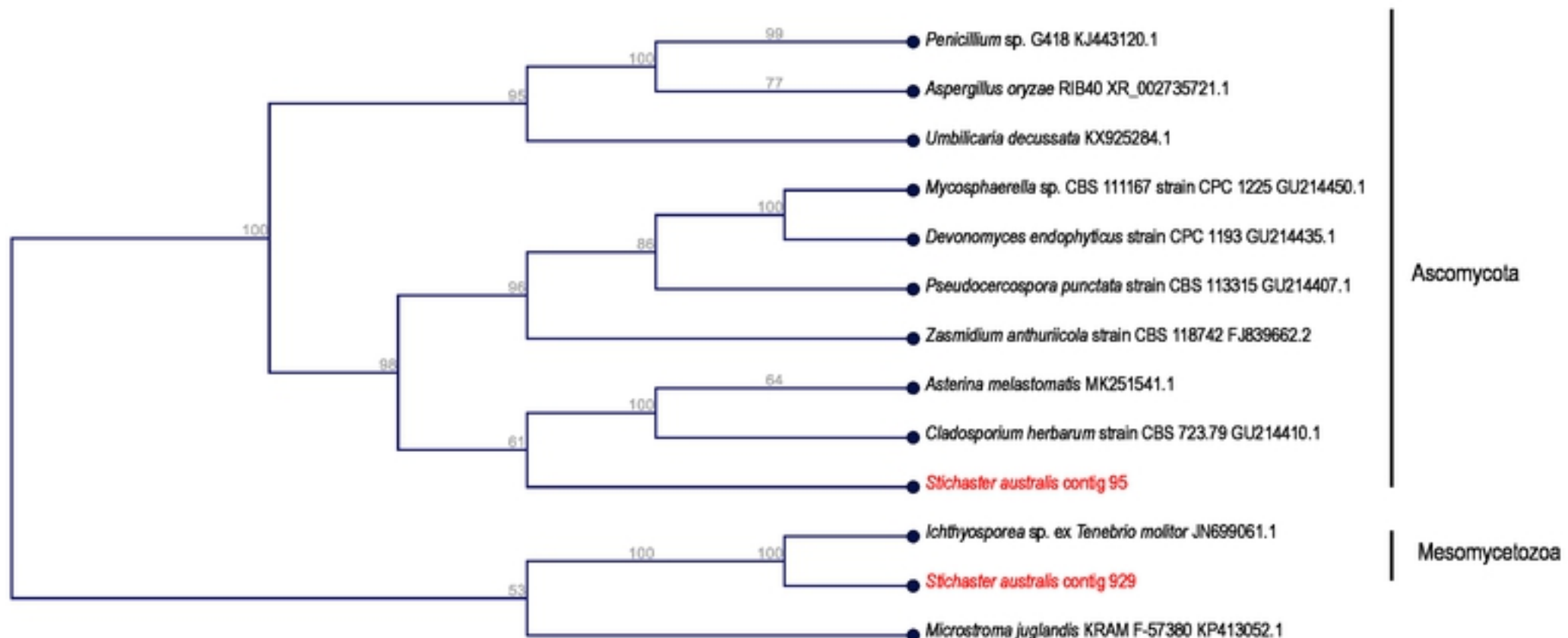


Figure 4

bioRxiv preprint doi: <https://doi.org/10.1101/2020.10.08.331132>; this version posted October 8, 2020. The copyright holder for this preprint (which was not certified by peer review) is the author/funder, who has granted bioRxiv a license to display the preprint in perpetuity. It is made available under aCC-BY 4.0 International license.

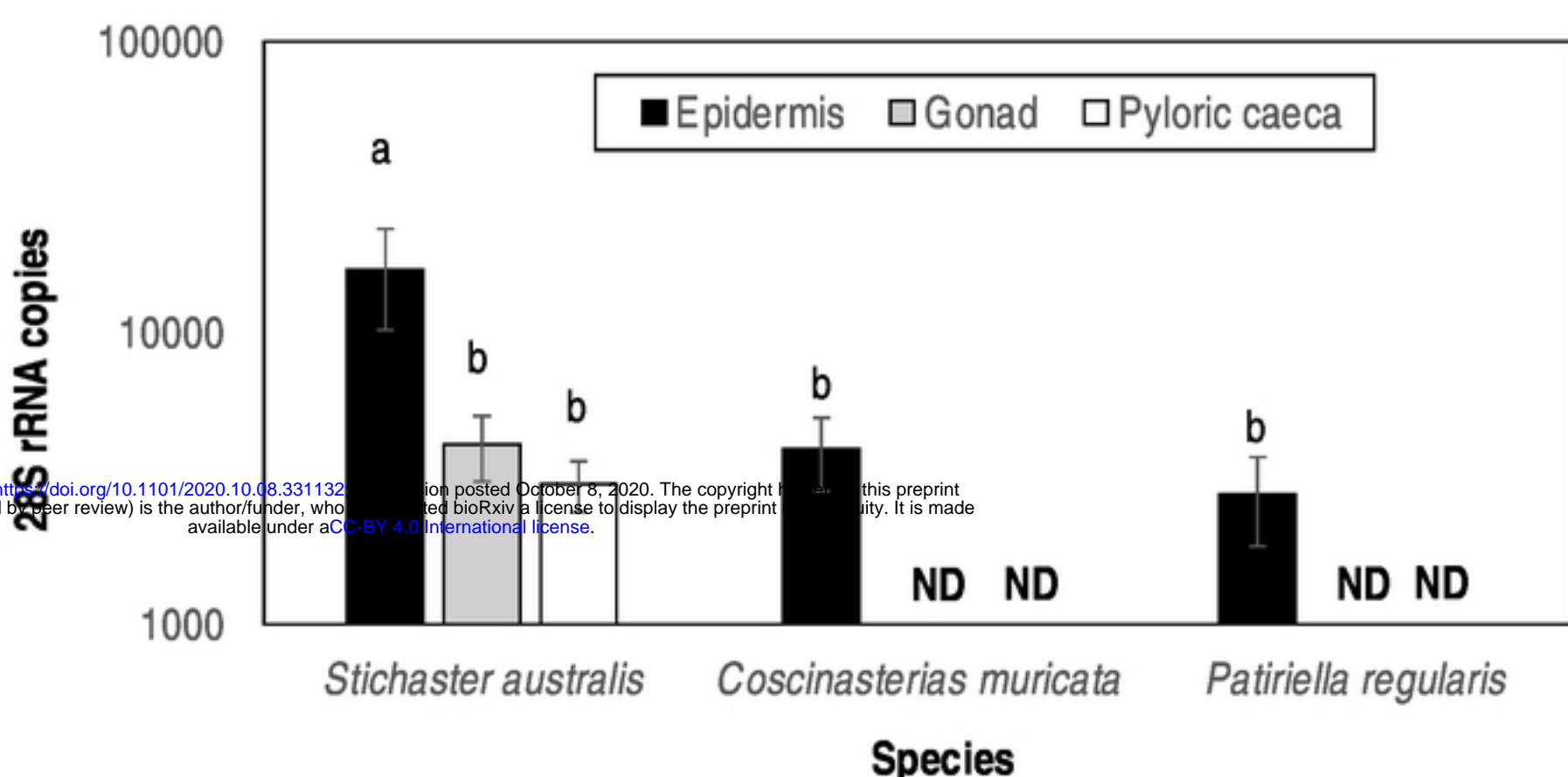


Figure 5